Modern Pathology (2020) 33:1702–1711
https://doi.org/10.1038/s41379-020-0539-7

ARTICLE

Papillary thyroid carcinoma with prominent myofibroblastic stromal component: clinicopathologic, immunohistochemical and next-generation sequencing study of seven cases

David Suster[1] · Michael Michal[2,3,4] · Michiya Nishino[1] · Simonetta Piana[5] · Massimo Bongiovanni[6] · Olga Blatnik[7] · Veronika Hájková[4] · Nikola Ptáková[4] · Michal Michal[2,4] · Saul Suster[8]

Received: 7 January 2020 / Revised: 23 March 2020 / Accepted: 24 March 2020 / Published online: 14 April 2020

Abstract

Papillary thyroid carcinoma with desmoid-type fibromatosis or nodular fasciitis-like stroma is an extremely unusual and poorly understood subtype of papillary thyroid cancer. Although prior studies have demonstrated alterations in the Wnt/β-catenin signaling pathway in some of these tumors, controversy still exists regarding the nature of the stromal spindle component. We have studied seven cases of papillary thyroid carcinoma with prominent myofibroblastic stroma, including six men and one woman aged 20–65 years (mean age = 44). All cases displayed areas consistent with conventional papillary thyroid carcinoma embedded in abundant myofibroblastic-like stroma. The myofibroblastic stroma in six cases resembled desmoid-type fibromatosis and in one case it more closely resembled nodular fasciitis. By immunohistochemical staining, the stromal spindle component showed positivity for SMA and low MIB1 proliferation index in all cases, and there was at least patchy strong nuclear positivity for beta-catenin in six/seven cases. Stains for cytokeratin AE1/AE3 and PAX8 were positive in the epithelial elements but negative in the stromal component. Next-generation sequencing was performed on six of seven cases. *CTNNB1* gene mutations were identified in six/seven cases. The epithelial component showed *BRAF* mutations in two cases and an *NRAS* mutation in one case. The case with fasciitis-like stroma was negative for beta-catenin by sequencing and immunostaining as well as negative for *USP6* gene rearrangement. Our findings indicate that papillary thyroid carcinoma with prominent myofibroblastic stroma may represent more than one category of lesions.

Introduction

Papillary thyroid carcinoma (PTC) is a common malignant neoplasm of the thyroid which may present with various morphologic appearances [1]. One rare variant, papillary thyroid carcinoma with desmoid-type fibromatosis (PTC-DTF) or fasciitis-like stroma (PTC-NFS) is characterized by conventional areas of PTC admixed with a prominent myofibroblastic component that is present in varying proportions. This subtype of PTC is not well defined and there are only ~30 cases reported to date in the literature. In the current 2017 edition of the WHO classification of Tumors of the Endocrine Organs, this entity is listed under the term "PTC with fibromatosis/fasciitis-like stroma" and is afforded only a short description [1]. Initial reports of this tumor type mostly referred to them as PTC with fasciitis like stroma [2–7]; however, additional studies, primarily in the form of case reports, have slowly been added to the body of literature under alternate designations including PTC with exuberant nodular fasciitis-like stroma, PTC forming

✉ Saul Suster
ssuster@mcw.edu

1 Department of Pathology, Beth Israel Deaconess Medical Center and Harvard Medical School, Boston, MA, USA

2 Department of Pathology, Charles University, Faculty of Medicine in Plzen, Plzen, Czech Republic

3 Biomedical Center, Charles University, Faculty of Medicine in Plzen, Plzen, Czech Republic

4 Bioptical Laboratory, Ltd., Plzen, Czech Republic

5 Pathology Unit, IRCCS - Arcispedale Santa Maria Nuova, Reggio Emilia, Italy

6 Institute of Pathology, Lausanne University Hospital, Lausanne, Switzerland

7 Department of Pathology, Institute of Oncology Ljubljana, Ljubljana, Slovenia

8 Department of Pathology, The Medical College of Wisconsin, Milwaukee, WI, USA

myofibroblastic nodular tumors and PTC with fibromatosis-like stroma [8–12]. More recently, additional reports and a few small series have demonstrated that many of these lesions are associated with *CTNNB1* (β-catenin) mutations [13–18]. Rebecchini et al. have suggested that these lesions be classified under the term papillary thyroid carcinoma with desmoid-type fibromatosis (PTC-DTF) for cases harboring *CTNNB1* mutations [14]. However, due to the rarity of these tumors, few cases have been examined with current sequencing techniques to corroborate the extent of *CTNNB1* mutations. Only a single case report exists with available next-generation sequencing (NGS) data in this tumor [18].

Herein we describe the clinicopathological characteristics of seven cases of papillary thyroid carcinoma with desmoid-type-fibromatosis/fasciitis-like stroma in which we examined immunohistochemical expression and molecular features by next-generation sequencing in the epithelial and mesenchymal components to better characterize the underlying genetic abnormalities driving these tumors. The majority of our cases had activating *CTNNB1* mutations identified consistent with the previously described PTC-DTF; however, one case in which the histology more closely resembled nodular fasciitis was negative for *CTNNB1* mutations. These findings indicate that there may be more than one subtype of PTC with myofibroblastic-type stroma.

Materials and methods

Owing to the rare nature of these lesions, the seven cases in this study were gathered primarily from the personal consultation files of the authors (MM, SS, OB, MB). One case was retrieved from the files at Beth Israel Deaconess Medical Center, Boston, MA. Cases which did not have available paraffin-embedded tissue blocks or which were not recent enough (>10 years old) to provide adequate quality genomic material were excluded. This study was conducted under IRB approval from the respective institutions. Of note, three of the seven cases examined were previously reported (Cases 1, 2, and 4) with two of the three cases undergoing molecular testing by pyrosequencing (Cases 2 and 4) [12, 13]. Case 1 was previously reported but did not undergo any molecular testing [12].

The histopathologic features of these seven cases were assessed using hematoxylin and eosin-stained sections (1–3 representative sections per case). The best available tissue blocks with both mesenchymal and epithelial components were selected for immunohistochemical and molecular analysis. Two cases which had previously undergone immunohistochemical testing or molecular testing by methods other than NGS were also included in the immunohistochemical and NGS analysis as part of the current study. Limited clinical and follow up data were available and thus only age, sex, tumor size, and location when available were recorded for each case.

Immunohistochemistry

Immunohistochemical studies were performed in six/seven cases. In one case (case 6), the tissue block was exhausted after sampling for molecular studies and thus could not be assessed for immunohistochemistry. Unstained tissue sections were cut from formalin-fixed paraffin-embedded (FFPE) blocks. Sections were deparaffinized in xylene, hydrated in descending dilutions of ethanol, and exposed to heat-induced epitope retrieval. Immunohistochemical analysis was performed using reagents from the Dako Envision FLEX kit (Agilent, Santa Clara, CA) and the Dako AutostainerPlus stainer (Agilent). Following pretreatment with Target Retrieval Solution (Agilent), tissue was blocked with peroxidase-blocking reagent for 5 min and incubated with the primary antibody at room temperature. Signals were detected using the Dako FLEX detection kit (Agilent). Counterstaining was performed with Envision FLEX (Agilent) hematoxylin for 7 min at room temperature. Appropriate positive and negative controls were run concurrently for all antibodies tested (Table 1). The immunohistochemical reaction was graded as positive based on nuclear, cytoplasmic or membrane reactivity for the various antibodies. Positivity was regarded as significant when it involved at least 50% of the tumor cell population.

Next-generation sequencing

NGS studies were performed on six/seven cases; one case (Case 4) had insufficient tumor cellularity for analysis of the mesenchymal component and four cases (Cases 1, 2, 3 and 4) had insufficient tumor cellularity for analysis of the epithelial component. In the one case with insufficient tissue for NGS analysis, the tumor had been studied previously by pyrosequencing. In the remaining cases, two to three FFPE sections (10 microns thick) were macrodissected to isolate tumor-rich regions. Samples were analyzed for the presence

Table 1 Antibody clones, manufacturer, and dilutions used for immunohistochemistry panel.

Antibody	Clone	Manufacturer	Dilution
Keratin AE1/AE3	AE1/AE3	Leica	Prediluted
MIB1	MIB-1	Dako	1:75
Beta Catenin	14/beta-catenin	Cell Marque	Prediluted
PAX8	MRQ-50	Cell Marque	Prediluted
SMA	Asm-1	Leica	Prediluted
P53	DO-7	Dako	1:50

Table 2 Clinicopathological characteristics of seven patients with PTC-DTF and PTC-NFS.

Case	Sex	Age	Location and size	Stromal features	Epithelial features
1	M	20	Left thyroid lobe 4.2 cm nodule with Infiltrative borders	Desmoid-type fibromatosis-like stroma Focal stromal edema	Conventional PTC with focal areas (<5%) displaying follicular architecture Limited epithelial component (<10%)
2	M	34	Right thyroid lobe 2.0 cm nodule with Focally infiltrative borders	Desmoid-type fibromatosis-like stroma Kelloidal type collagen fibers	Conventional PTC Limited epithelial component (<5%)
3	M	53	Left thyroid lobe 3.6 cm nodule Focally infiltrative borders	Desmoid-type fibromatosis-like stroma	Conventional PTC Limited epithelial component (<10%)
4	M	48	Right thyroid lobe 2.8 cm nodule Focally infiltrative borders	Desmoid-type fibromatosis-like stroma	Conventional PTC Limited epithelial component (<15%)
5	M	65	Location and size unknown Infiltrative borders	Nodular Fasciitis-like stroma Prominent stromal edema Mucin pools	Conventional PTC Epithelial component prominent (~50%)
6	M	58	Left thyroid Lobe Size unknown.	Desmoid-type fibromatosis-like stroma	Follicular variant of papillary thyroid carcinoma
7	F	30	Location and size unknown. Focally infiltrative borders	Desmoid-type fibromatosis-like stroma	Conventional PTC Limited epithelial component (30%)

PTC papillary thyroid carcinoma, *PTC-DTF* papillary thyroid carcinoma with desmoid-type fibromatosis-like stroma, *PTC-NFS* papillary thyroid carcinoma with nodular fasciitis-like stroma.

of common molecular alterations in thyroid and lung cancer including gene fusions, single nucleotide variants, indels and splice-site alterations by targeted sequencing with the Archer FusionPlex comprehensive thyroid and lung (CTL) panel (ArcherDX Inc.) as previously described [19]. Fusions in genes including *ALK*, *AXL*, *BRAF*, *CCND1*, *EGFR*, *FGFR1*, *FGFR2*, *FGFR3*, *MET*, *NRG1*, *NTRK1*, *NTRK2*, *NTRK3*, *PPARGH*, *RAF1*, *RET*, *ROS1*, *THADA* were analyzed, as well as point mutations in the hotspot regions of genes including: *AKT1*, *ALK1*, *BRAF*, *CTNNB1*, *DDR2*, *EGFR*, *ERBB2*, *FGFR1*, *GNAS*, *HRAS*, *IDH1*, *IDH2*, *KRAS*, *MAP2K1*, *NRAS*, *PIK3CA*, *RET*, *and ROS1*. A single case that morphologically resembled nodular fasciitis, and which was negative for *CTNNB1* mutations with this panel was tested a second time with an alternate NGS panel covering *USP6* rearrangements (Archer FusionPlex Sarcoma Panel, ArcherDX, San Diego, CA) as previously described [20]. For all cases, libraries were sequenced on a NextSeq 500 sequencer (Illumina, San Diego, CA). Analysis of sequencing results was performed using the Archer Analysis software (v5; ArcherDX Inc.). Fusion parameters were set to a minimum of five valid fusion reads with a minimum of three unique start sites within the valid fusion reads.

Results

Clinical features

The clinical features of our patients are presented in Table 2. The patients included six men and one woman aged 20–65 years (mean age = 44). Patients presented primarily with a neck mass with vaguely circumscribed borders. Tumors ranged in size from 2.0 to 4.2 cm in diameter. Complete clinical histories were not available for all patients; however, in at least three cases (Cases 1, 2, and 4) pre-surgical fine-needle aspirations were performed, of which was diagnostic of PTC, one of which was suspicious for PTC, and one of which was reported as atypical [12, 13]. One case (Case 3) was received in consultation to rule out a spindle cell component of anaplastic carcinoma.

Histopathologic features

The histologic features of the stromal and epithelial components are summarized in Table 2. Histological examination demonstrated that all the cases showed a biphasic, mixed epithelial-mesenchymal composition. In

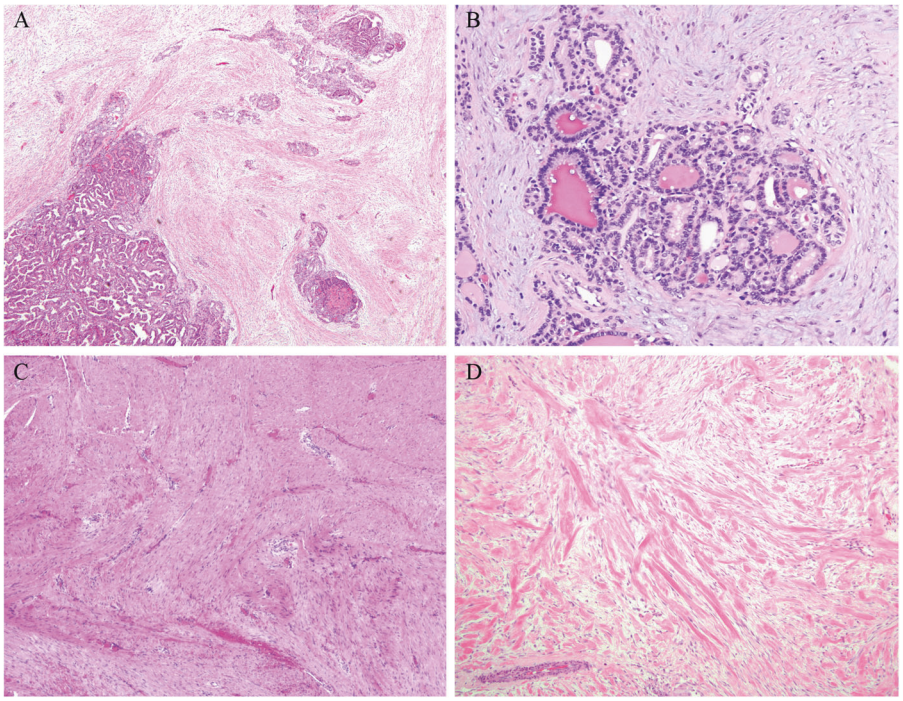

Fig. 1 Papillary thyroid carcinoma with desmoid-type fibromatosis showing. a Islands of classical papillary thyroid carcinoma surrounded by desmoid-type fibromatosis (case 1); **b** Islands of follicular patterned thyroid carcinoma (follicular variant of papillary thyroid carcinoma) surrounded by a fibroblastic appearing spindle cell proliferation (case 6); **c** Higher magnification from stromal component (Case 3) showing fascicles of bland-appearing spindle cells with evenly distributed nuclei embedded in a collagenous stroma; **d** Large keloidal collagen fibers seen separating the spindle cells were seen in one case (Case 2).

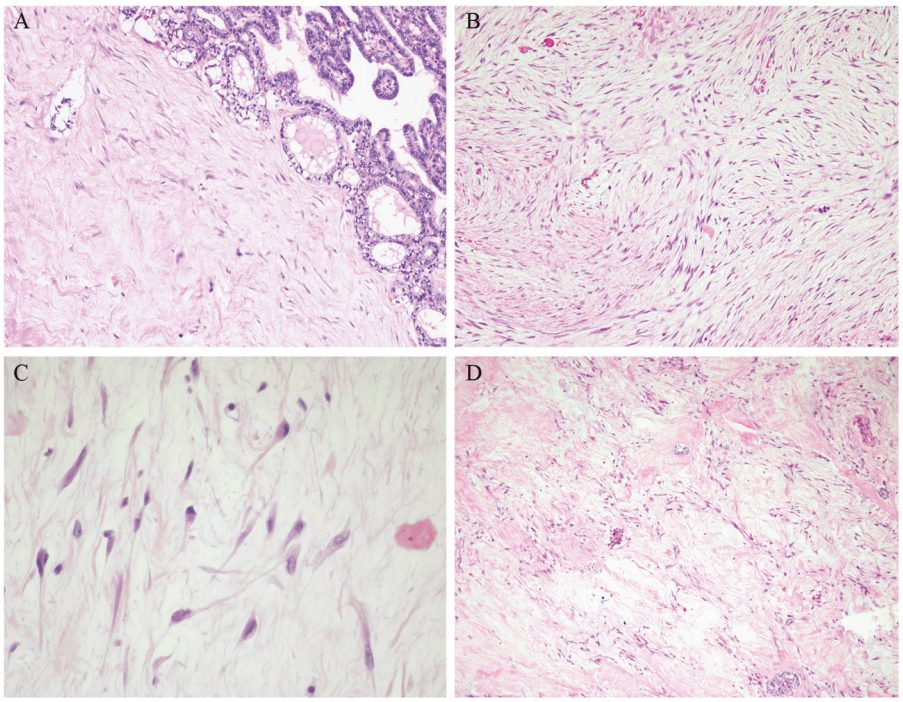

Fig. 2 Papillary thyroid carcinoma with nodular fasciitis-like stroma (Case 5) showing. a A conventional papillary thyroid carcinoma with a sparse spindle cell proliferation with edematous stroma; **b** In some areas, the spindle cell proliferation adopted a vaguely storiform growth pattern; **c** Areas showed spindle and stellate cells with long cytoplasmic processes against an edematous background reminiscent of granulation tissue; **d** Other areas displayed abundant pools of stromal mucin.

five of seven cases (cases 1–4, and case 7) conventional PTC was present in association with a prominent myofibroblastic component resembling desmoid-type fibromatosis. In one case (case 6) the follicular variant of papillary thyroid carcinoma was present in association with desmoid-type fibromatosis-like stroma. In one case (Case 5) conventional PTC was present in association with nodular fasciitis-like stroma. On scanning magnification of the PTC-DTF cases, the stromal component contained elongated and intersecting fascicles of evenly dispersed bland-appearing spindle cells with scattered small vessels and scattered epithelial elements (Fig. 1a). The entrapped islands of neoplastic epithelium in five of seven cases showed the features of classical papillary thyroid carcinoma, with papillary tufts and follicles lined by cells with enlarged nuclei, clearing of the

Table 3 Immunohistochemical and molecular genetic findings in seven patients with PTC-DTF and PTC-NFS.

Case	Myofibroblastic stroma IHC	PTC IHC	Molecular
1	Beta Catenin + (Nuclear) Keratin AE1/AE3− MIB1 < 5% PAX8− P53− SMA+	Beta Catenin + (Membranous) Keratin AE1/AE3+ MIB1 < 5% PAX8+ P53− SMA−	*CTNNB1* c.121A>G, (p.Thr41Ala)
2	Beta Catenin + (Nuclear) Keratin AE1/AE3− MIB1 < 5% PAX8− P53− SMA+	Beta Catenin + (Membranous) Keratin AE1/AE3+ MIB1 < 5% PAX8+ P53− SMA−	*CTNNB1* c.133T>C, (p.Ser45Pro) Epithelial component not available for testing, however previously tested [13] and positive for *BRAF* c.1799T>A (p.Val600Glu)
3	Beta Catenin + (Nuclear) Keratin AE1/AE3− MIB1 < 5% PAX8− P53− SMA+	Beta Catenin + (Membranous) Keratin AE1/AE3+ MIB1 < 5% PAX8+ P53− SMA−	*CTNNB1* c.124A>G, (p.Thr41Ala)
4	Beta Catenin + (Nuclear) Keratin AE1/AE3− MIB1 < 5% PAX8− P53− SMA+	Beta Catenin + (Membranous) Keratin AE1/AE3+ MIB1 < 5% PAX8+ P53− SMA−	Failed repeat sequencing/QNS, However, epithelial and mesenchymal component previously tested and reported positive [13] for: *CTNNB1* c.133T>C (p.Ser45Pro) *BRAF* c.1799T>A (p.Val600Glu)
5	Beta Catenin − (Nuclear) Keratin AE1/AE3− MIB1 ~5–10% PAX8− P53− SMA+	Beta Catenin + (Membranous) Keratin AE1/AE3+ MIB1 < 5% PAX8+ P53− SMA−	*BRAF* c.1799T>A, (p.Val600Glu) *USP6* rearrangement negative by NGS
6	Tissue exhausted	Tissue exhausted	*CTNNB1* c.121A>G, (p.Thr41Ala) *NRAS* c.175G>A, (p.Ala59Thr)
7	Beta Catenin + (Nuclear) Keratin AE1/AE3− MIB1 < 5% PAX8− P53− SMA+	Beta Catenin + (Membranous) Keratin AE1/AE3+ MIB1 < 5% PAX8+ P53− SMA−	*CTNNB1* c.134C>T, (p.Ser45Phe) *BRAF* c.1799T>A, (p.Val600Glu)

NGS next-generation sequencing, *IHC* immunohistochemistry, *QNS* quantity not sufficient.

nuclear chromatin and longitudinal nuclear grooves. In one case, the epithelial component showed no evidence of papillary architecture consistent with the follicular variant of papillary thyroid carcinoma (Fig. 1b). On higher magnification, the stromal component showed an orderly, evenly spaced proliferation of bland spindle cells embedded in a collagenous stroma (Fig. 1c). In one case (case 2), thickened, keloidal-type collagen fibers could be seen separating the spindle cells (Fig. 1d). No increased mitotic activity or necrosis was identified in any of these cases, either in the spindle or epithelial components. In six/seven cases, infiltration of the surrounding structures could also be identified at least focally. In all the lesions with desmoid-type fibromatosis the mesenchymal component was dominant ranging from 70% to >90%. One case (Case 5) contained a spindle stromal component that more closely resembled nodular fasciitis and was characterized by a sparsely cellular proliferation of bland-appearing spindle to stellate cells embedded in a loose edematous matrix (Fig. 2a). In areas, the spindle cells adopted a vaguely storiform configuration (Fig. 2b). The spindle cells were devoid of significant nuclear atypia and

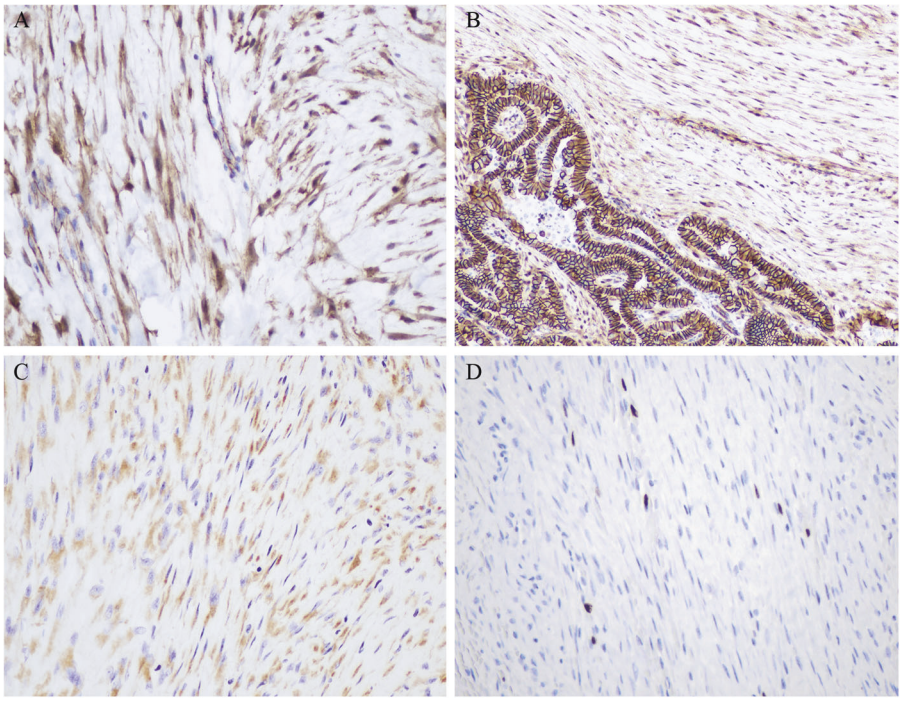

Fig. 3 Immunohistochemistry in PTC-DTF and PTC-NFS. **a** Immunohistochemical staining of the stromal component for beta-catenin showed nuclear and cytoplasmic staining in the spindle cells of PTC-DTF; **b** Small island of neoplastic epithelium showing strong membranous staining for beta-catenin in the PTC tumor cells as well as in the spindle cells in the surrounding stroma; **c** Spindle cells in the stroma showed cytoplasmic staining for SMA in both cases of PTC-DTF and PTC-NFS, supporting a myofibroblastic phenotype; **d** MIB1 immunostaining showed scattered nuclear positivity in a few of the nuclei in PTC-NFS (Case 5).

Fig. 4 The genotype-phenotype associations of the 7 cases of PTC-DTF and PTC-NFS are shown. The histologic features of each case are displayed across the top two rows and the molecular alterations are displayed below. The lighter boxes represent alterations which were identified in a prior study.

no areas of necrosis were identified in this case. In a few areas, the spindle cells focally adopted a stellate configuration resembling a tissue culture-like pattern (Fig. 2c). Pools of stromal mucin were also present (Fig. 2d) along with extravasated red blood cells and focal inflammatory lymphoid infiltrates. The PTC component, in this case, was the most extensive of all cases examined and comprised ~50% of the tumor.

Immunohistochemical features

A limited immunohistochemical panel of stains including keratin AE1/AE3, MIB1, PAX8, P53, beta catenin, and SMA was performed on six cases and is presented in Table 3. The PTC component showed strong, diffuse membranous staining for keratin AE1/AE3 and nuclear staining for PAX8 in all cases examined; neither of these markers stained the spindle-cell component of the tumor. All five cases with fibromatosis-like stroma showed at least focal nuclear staining for beta-catenin in the spindle-cell component (Fig. 3a); these cases also demonstrated cytoplasmic staining for beta catenin to varying degrees of intensity and extent. Beta-catenin immunostaining of the single case with nodular fasciitis-like stroma showed scattered cytoplasmic staining without nuclear expression. In addition, beta catenin showed membranous staining of the epithelial component in all the tumors (Fig. 3b). SMA was positive in all cases within the mesenchymal spindle cell component and negative in the epithelial component (Fig. 3c). MIB1 immunostaining in all the tumors showed low proliferation indexes (<5%) in the stromal component of PTC-DTF as well as PTC-NFS, although it was overall slightly more elevated in the PTC-NFS case (Fig. 3d). P53 was negative (wild-type staining pattern) in all cases in both the mesenchymal and epithelial components.

Molecular genetic features

The molecular genetic features of the seven cases studied are summarized in Table 3 and Fig. 4. NGS using a targeted, commercially available panel (Archer FusionPlex Comprehensive Thyroid and Lung panel) was successfully applied to the mesenchymal component in six/seven cases (Table 2). One of the seven cases (Case 4) failed sequencing due to suboptimal quantity of the input material; however, this case was previously reported to have a *CTNNB1* c.133T>C (p.Ser45Pro) mutation by pyrosequencing [13]. Of the six cases with adequate material, five were positive for *CTNNB1* mutations, all of which were histologically classified as PTC-DTF. Three cases showed a *CTNNB1* c.121A>G (p.Thr41Ala) mutation; one case showed a *CTNNB1* c.133T>C (p.Ser45Pro) mutation, and one case showed a *CTNNB1* c.134C>T (p.Ser45Phe) mutation. The single case negative for *CTNNB1* mutations was histologically distinct and was classified as PTC-NFS. This case was also negative for *USP6* rearrangements using a second NGS panel with coverage for *USP6* rearrangements.

NGS of the epithelial component was successfully performed in three/seven cases. Cases 1, 2, 3 and 4 did not contain sufficient cellularity of the epithelial component for NGS, either due to low initial tumor cellularity or due to exhaustion of the tissue for prior testing. Two *BRAF* c.1799T>A (p.Val600Glu) mutations were identified and one case (Case 7) showed an *NRAS* c.175G>A, (p.Ala59Thr) mutation. In addition, two of the four cases (Cases 2 and 4) with insufficient tumor cellularity for NGS study had undergone prior pyrosequencing which identified *BRAF* c.1799T>A (p.Val600Glu) mutations in the epithelial component [13].

In summary, incorporating the results of the two previously reported cases included in this study, the stromal component was evaluated in seven cases; six/six (100%) cases with desmoid-type fibromatosis-like stroma were positive for *CTNNB1* mutations, while the single case with nodular fasciitis-like stroma was negative for *CTNNB1* mutations and *USP6* gene rearrangements. The most common mutation identified was the *CTNNB1* c.121A>G, (p.Thr41Ala) mutation which was present in three/six (50%) cases with desmoid-type fibromatosis-like stroma. The epithelial component was evaluated in five/six cases; *BRAF* c.1799T>A (p.Val600Glu) was present four/five cases (3 PTC-DTF, 1 PTC-NFS). One case (Case 7) showed an *NRAS* c.175G>A, (p.Ala59Thr) mutation. Two cases had insufficient tumor cellularity for NGS and no prior history of molecular testing for the epithelial component.

Discussion

Papillary thyroid carcinoma with desmoid-type fibromatosis or nodular fasciitis-like stroma represent rare variants of PTC [1]. These tumors are composed of mixed epithelial and mesenchymal elements with a predominance of the mesenchymal component in nearly all cases and usually only small islands of PTC scattered throughout. In addition, the mesenchymal component often forms a discrete mass which often grows and infiltrates independent of the associated epithelial malignancy. This feature, amongst others, separates these lesions from the desmoplastic stromal response that commonly occurs in PTC [21]. Although rare, epithelial malignancies with associated fibromatosis-like or fasciitis-like stroma have also been reported in other organ systems and may constitute a potential pitfall for diagnosis [22, 23].

In our study, six of seven cases corresponded to the desmoid-type fibromatosis variant (PTC-DTF), while one case more closely resembled nodular fasciitis and was classified as a nodular fasciitis-like variant (DTF-NFS). While rare, recognition of PTC with these particular stromal features is of importance due to the occurrence of other benign and malignant processes in the thyroid that may have a spindle cell appearance, including benign or reactive processes such as the fibrous variant of Hashimoto's thyroiditis, Riedel's thyroiditis, post-operative spindle cell nodules, and scarring following fine-needle aspiration

procedures, as well as some neoplastic entities which may contain a spindle cell component including anaplastic thyroid carcinoma, medullary thyroid carcinoma and other mesenchymal spindle cell neoplasms [24–28]. In addition to this, sampling issues at the time of biopsy or fine-needle aspiration as well as unfamiliarity with this presentation of PTC may lead to diagnostic difficulties [29]. While extensive clinical information was not available for all the cases in our study, at least one of the cases was received in consultation with concern for spindle cell anaplastic carcinoma, and in two cases pre-surgical fine-needle aspirations had to be repeated because of lack of diagnostic material. In a recent study, one case of PTC-DTF was initially diagnosed as a schwannoma, while a second case was initially diagnosed as fibroma [16]. Thus, awareness of this particular entity may allow for more accurate diagnosis and more efficient management of patients with these tumors.

Immunohistochemically, all the cases in this study displayed some degree of staining for beta-catenin in the mesenchymal component. The staining for beta-catenin was both nuclear and cytoplasmic. Although most cases showed convincing and strong nuclear staining for beta-catenin, the staining was mostly focal and patchy. Despite these findings, one study has reported lack of beta-catenin staining in one of these tumors [18]. The authors of this report also found that the stromal compartment in their particular case was positive for SOX11, a nuclear transcription factor which has also been shown to be positive in some cases of desmoid-type fibromatosis [30]. However, given that the majority of these lesions seem to be associated with *CTNNB1* mutations and a high proportion have shown expression of beta-catenin by IHC we feel that beta-catenin should be the first diagnostic marker ordered for the evaluation of potential cases of these tumors [12, 13, 16, 18]. IHC for keratin, P53 and PAX8 is of importance as well, since the spindled mesenchymal component in these tumors should have a negative staining pattern for these markers; while anaplastic carcinoma may be negative for these stains in some cases, positivity within the mesenchymal component should raise suspicion for an anaplastic carcinoma component. This distinction is especially important considering that anaplastic thyroid carcinoma represents an exceedingly aggressive neoplasm, while PTC-DTF and PTC-NFS follow a generally favorable course when managed similar to conventional papillary thyroid carcinoma [31].

Genetically these tumors seem to fall into two separate subcategories; the first is PTC-DTF which is characterized by activating *CTNNB1* mutations, the second is PTC-NFS which as of this time has not been found to have any associated genetic alterations. The *CTNNB1* gene encodes for β-catenin; a protein involved in the transmission of extracellular signals via the Wnt/β-catenin signaling pathway. Mutations in Exon 3 of *CTNNB1* have been described extensively in human cancers and are known to drive tumorigenesis in numerous tumors including desmoid-type fibromatosis [32, 33]. In the thyroid, only the cribriform morular variant of PTC has been shown so far to be associated with *CTNNB1* mutations [34]. *CTNNB1* mutations have been identified in 5/12 cases of PTC with DTF/NFS thus far [13, 15, 17, 18]. The largest prior molecular analysis by Takada et al. [15] was only able to identify *CTNNB1* mutations in one of eight cases tested, despite positive beta-catenin staining by IHC in the majority of their cases. They concluded that an alternate mechanism might play a role in activation of the Wnt/β-catenin signaling pathway [15]. However, that study was conducted via direct sequencing using capillary electrophoresis, which has a lower limit of detection than NGS, and orthogonal methods were not used to exclude false negatives. The lower sensitivity of that assay may account for the negative results seen in their cases. In our study using a more sensitive NGS platform we were able to identify *CTNNB1* mutations in 100% (six of six) of our cases of PTC-DTF using a targeted panel indicating that activating mutations of *CTNNB1* are in fact common and likely the molecular drivers of the fibroblastic proliferation in the majority of these tumors. The three mutations identified in our cohort included *CTNNB1* c.121A>G, p. (Thr41Ala), c.133T>C, p.(Ser45Pro), and *CTNNB1* c.134C>T, p.(Ser45Phe) consistent with previously reported mutations in these tumors [13, 15, 17, 18]. In desmoid-type fibromatosis the presence of a particular *CTNNB1* mutation, the Ser45Phe mutation, has been shown to be correlated with an increased risk of recurrence [35]; however too few cases of PTC-DTF/NFS with available clinical follow up currently exist to accurately assess the effect of specific mutations on prognosis and behavior in the thyroid gland.

For now, cases of PTC with nodular fasciitis-like stroma have no known molecular alterations which may act as drivers within the stromal compartments. While *MYH9-USP6* rearrangements have been described to occur in up to 90% of nodular fasciitis cases in soft tissue [36–38], we were unable to demonstrate any evidence of *USP6* rearrangement by NGS in our case. An alternative hypothesis could be that the stromal proliferation in such cases is driven by the presence of the *BRAF* mutations [18]. Activating *BRAF* mutations are the most common driver mutations identified in papillary thyroid carcinoma, with the *BRAF* Val600Glu mutation being the most common [1, 39]. Studies have shown that the presence of *BRAF* mutations may increase the amounts of associated myofibroblastic stroma in cases of PTC [40]. In our study, we confirm the presence of *BRAF* c.1799T>A (p.Val600Glu) mutations within PTC-DTF and PTC-NFS cases. In addition, nearly every mutation reported to date in PTC-DTF/NFS has been a *BRAF*

Val600Glu mutation [13, 15, 17, 18]. A single case report of PTC-DTF identified a *BRAF* c.1799_1801delTGA (p.Val600_Lys601delinsE) mutation [18]; which has also been rarely reported in conventional PTC [41]. Herein, we also report the first instance of a driver mutation other than *BRAF*; a single *NRAS* c.175G>A, (p.Ala59Thr) mutation in the epithelial component of a PTC-DTF case. Coincidentally this *NRAS* mutation corresponded to the single case in our study which showed the follicular variant of papillary thyroid carcinoma rather than classical papillary type suggesting that the stromal proliferation in these lesions is not strictly associated with a particular variant of PTC. Although our sample size is low, the high proportion of *BRAF* mutations in these cases is in keeping with the reported frequency of *BRAF* alterations in conventional PTC [1]. While the mesenchymal proliferation in PTC-DTF is likely driven by *CTNNB1* activating mutations, whether the stroma in PTC-NFS represents a neoplastic or reactive proliferation driven by mutations in the adjoining epithelial malignancy remains to be determined.

In summary, we have examined the clinicopathologic, immunohistochemical and molecular genetic features of seven cases of PTC-DTF/NFS. Our study represents the largest NGS study of these lesions to date and confirms that *CTNNB1* activating mutations are the driver events behind PTC-DTF. We believe cases of PTC containing myofibroblastic stroma with beta-catenin expression by IHC and *CTNNB1* mutations by NGS represent a distinct clinicopathologic entity that pathologists and clinicians should be aware of. In addition, our findings indicate that there appears to be a subcategory of PTC with myofibroblastic-like stroma without beta-catenin expression or mutations, which more closely resembles nodular fasciitis than desmoid-type fibromatosis. Whether the myofibroblastic proliferation in this subcategory of PTC represents a reactive or neoplastic process requires additional investigation.

Acknowledgements The authors would like to thank Christopher Green for the creation of Fig. 4.

Compliance with ethical standards

Conflict of interest The authors declare that they have no conflict of interest.

References

1. Lloyd R, Osamura R, Kloppel G. WHO classification of tumors of endocrine organs. Lyon, France: IARC Press; 2017.
2. Michal M, Chlumska A, Fakan F. Papillary carcinoma of thyroid with exuberant nodular fasciitis-like stroma. Histopathology. 1992;21:577–9.
3. Chan JK, Carcangiu ML, Rosai J. Papillary carcinoma of thyroid with exuberant nodular fasciitis-like stroma. Report of three cases. Am J Clin Pathol. 1991;95:309–14.
4. Chan JK. Papillary carcinoma of thyroid: classical and variants. Histol Histopathol. 1990;5:241–57.
5. Mizukami Y, Nonomura A, Matsubara F, Michigishi T, Ohmura K, Hashimoto T. Papillary carcinoma of the thyroid gland with fibromatosis-like stroma. Histopathology. 1992;20:355–7.
6. Mizukami Y, Kurumaya H, Kitagawa T, Minato H, Nonomura A, Michigishi T, et al. Papillary carcinoma of the thyroid gland with fibromatosis-like stroma: a case report and review of the literature. Mod Pathol. 1995;8:366–70.
7. Naganuma H, Iwama N, Nakamura Y, Ohtani N, Ohtani H, Takaya K, et al. Papillary carcinoma of the thyroid gland forming a myofibroblastic nodular tumor: report of two cases and review of the literature. Pathol Int. 2002;52:54–8.
8. Wu Z, Chu X, Fan S, Meng X, Xu C. Papillary thyroid carcinoma with fibromatosis-like stroma: a case report and review of the literature. Oncol Lett. 2013;5:215–7.
9. Inaba M, Umemura S, Satoh H, Ichikawa Y, Abe Y, Kirokawa K, et al. Papillary thyroid carcinoma with fibromatosis-like stroma: a report of two cases. Endocr Pathol. 2002;13:219–25.
10. Toti P, Tanganelli P, Schürfeld K, Stumpo M, Barbagli L, Vatti R, et al. Scarring in papillary carcinoma of the thyroid: report of two new cases with exuberant nodular fasciitis-like stroma. Histopathology. 1999;35:418–22.
11. Terayama K, Toda S, Yonemitsu N, Koike N, Sugihara H. Papillary carcinoma of the thyroid with exuberant nodular fasciitis-like stroma. Virchows Arch. 1997;431:291–5.
12. Roth EM, Barrows CE, Nishino M, Sacks B, Hasselgren PO, James BC. Papillary thyroid cancer with extrathyroidal extension of desmoid-type fibromatosis. A case report of an aggressive presentation of an uncommon pathologic entity. Int J Surg Case Rep. 2019;63:5–9.
13. Rebecchini C, Nobile A, Piana S, Sarro R, Bisig B, Gerasimos SP, et al. Papillary thyroid carcinoma with nodular fasciitis-like stroma and β-catenin mutations should be renamed papillary thyroid carcinoma with desmoid-type fibromatosis. Mod Pathol. 2017;30:236–45.
14. Tajiri K, Hirokawa M, Suzuki A, Takada N, Ota H, Oshita M, et al. Can Ultrasound alone predict papillary thyroid carcinoma with desmoid-type fibromatosis? A retrospective analysis of 13 cases, focusing on the stromal area. Ultrasound Int Open. 2018;4:E39–44.
15. Takada N, Mussazhanova Z, Hirokawa M, Nakashima M, Miyauchi A. Immunohistochemical and molecular analyses focusing on mesenchymal cells in papillary thyroid carcinoma with desmoid-type fibromatosis. Pathobiology. 2018;85:300–3.
16. Takada N, Hirokawa M, Ito M, Suzuki A, Higuchi M, Kuma S, et al. Papillary thyroid carcinoma with desmoid-type fibromatosis: a clinical, pathological, and immunohistochemical study of 14 cases. Endocr J. 2017;64:1017–23.
17. Zhou L, Shi L, Jiang Z, Xie L. Papillary thyroid carcinoma with nodular fasciitis-like stroma and B-catenin gene mutations: report of a recurrent case. Int J Clin Exp Pathol. 2018;11:2879–83.
18. Wong SBJ, Nga ME, Michal M, Vanecek T, Seet JE, Petersson F. SOX11 expression in a case of papillary thyroid carcinoma with fibromatosis/fasciitis-like stroma containing BRAF c.1799_1801delTGA and CTNNB1 c.133T>C mutations. Virchows Arch. 2019;475:519–25.
19. Skalova A, Vanecek T, Martinek P, Weinreb I, Stevens TM, Simpson RHW, et al. Molecular profiling of mammary analog secretory carcinoma revealed a subset of tumors harboring a novel

ETV6-RET translocation; report of 10 cases. Am J Surg Path. 2018;42:234–46.
20. Svajdler M, Michal M, Martinek P, Ptakova N, Kinkor Z, Szepe P, et al. Fibro-osseous pseudotumor of digits and myositis ossificans show consistent *COL1A1-USP6* rearrangement: a clinicopathological and genetic study of 27 cases. Hum Pathol. 2019;88:39–47.
21. Cho JG, Byeon HK, Oh KH, eBaek SK, Kwon SY, Jung KY, et al. Clinicopathological significance of cancer-associated fibroblasts in papillary thyroid carcinoma: a predictive marker of cervical lymph node metastasis. Eur Arch Otorhinolaryngol. 2018;275:2355–6231.
22. Tajima S, Takanashi Y, Koda K. Squamous cell carcinoma of the lung with highly proliferating fibromatosis-like stroma: a rare phenomenon. Int J Clin Exp Pathol. 2015;8:5870–6.
23. Švajdler M, Michal M, Dubinsky P, Svajdler P, Ondic O, Michal M. Endometrial endometrioid carcinoma with large cystic growth configuration and deceptive pattern of invasion associated with abundant nodular fasciitis-like stroma: a unique hitherto unreported histology in endometrioid carcinoma. Adv Anat Pathol. 2016;23:381–4.
24. Brandwein-Gensler MS, Wang BY, Urken ML. Spindle cell transformation of papillary carcinoma: an aggressive entity distinct from anaplastic thyroid carcinoma. Arch Pathol Lab Med. 2004;128:87–9.
25. Kim SW, Oh YL, Choi JY, Lee JI, Chung JH, Kim JS. Postoperative spindle cell nodule after thyroidectomy: a case mimicking recurrence with anaplastic transformation of thyroid cancer. Head Neck. 2013;35:E13–7.
26. Thompson LDR, Wei C, Rooper LM, Lau SK. Thyroid gland solitary fibrous tumor: report of 3 cases and a comprehensive review of the literature. Head Neck Pathol. 2019;13:597–605.
27. Papi G, Corrado S, LiVolsi VA. Primary spindle cell lesions of the thyroid gland; an overview. Am J Clin Pathol. 2006;125:S95–123.
28. Ragazzi M, Ciarrocchi A, Sancisi V, Gandolfi G, Bisagni A, Piana S. Update on anaplastic thyroid carcinoma: morphological, molecular, and genetic features of the most aggressive thyroid cancer. Int J Endocrinol. 2014;2014:790834.
29. Yang YJ, LiVolsi VA, Khurana KK. Papillary thyroid carcinoma with nodular fasciitis-like stroma. Pitfalls in fine-needle aspiration cytology. Arch Pathol Lab Med. 1999;123:838–41.
30. Misemer BS, Skubitz AP, Carlos Manivel J, Schmechel SC, Cheng EY, Henriksen JC, et al. Expression of FAP, ADAM12, WISP1, and SOX11 is heterogeneous in aggressive fibromatosis and spatially relates to the histologic features of tumor activity. Cancer Med. 2014;3:81–90.
31. Basu S, Nair N, Shet T, Borges AM. Papillary thyroid carcinoma with exuberant nodular fasciitis-like stroma: treatment outcome and prognosis. J Laryngol Otol. 2006;120:338–42.
32. Gao C, Wang Y, Broaddus R, Sun L, Xue F, Zhang W. Exon 3 mutations of CTNNB1 drive tumorigenesis: a review. Oncotarget. 2017;9:5492–508.
33. Le Guellec S, Soubeyran I, Rochaix P, Filleron T, Neuville A, Hostein I, et al. CTNNB1 mutation analysis is a useful tool for the diagnosis of desmoid tumors: a study of 260 desmoid tumors and 191 potential morphologic mimics. Mod Pathol. 2012;25:1551–8.
34. Lam AKY, Saremi N. Cribriform-morular variant of papillary thyroid carcinoma: a distinctive type of thyroid cancer. Endocr Relat Cancer. 2017;24:R109–21.
35. Lazar AJ, Tuvin D, Hajibashi S, Habeeb S, Bolshakov S, Mayordomo-Aranda E, et al. Specific mutations in the beta-catenin gene (CTNNB1) correlate with local recurrence in sporadic desmoid tumors. Am J Pathol. 2008;173:1518–27.
36. Patel NR, Chrisinger JSA, Demicco EG, Sarabia SF, Reuther J, Kumar E, et al. USP6 activation in nodular fasciitis by promoter-swapping gene fusions. Mod Pathol. 2017;30:1577–88.
37. Erber R, Agaimy A. Misses and near misses in diagnosing nodular fasciitis and morphologically related reactive myofibroblastic proliferations: experience of a referral center with emphasis on frequency of USP6 gene rearrangements. Virchows Arch. 2018;473:351–60.
38. Shin C, Low I, Ng D, Oei P, Miles C, Symmans P. USP6 gene rearrangement in nodular fasciitis and histological mimics. Histopathology. 2016;69:784–91.
39. Zou M, Baitei EY, Alzahrani AS, BinHumaid FS, Alkhafaji D, Al-Rijjal RA, et al. Concomitant RAS, RET/PTC, or BRAF mutations in advanced stage of papillary thyroid carcinoma. Thyroid. 2014;24:1256–66.
40. Tarabichi M, Antoniou A, Le Pennec S, Gacquer D, de Saint Aubain N, Craciun L, et al. Distinctive desmoplastic 3D morphology associated with BRAFV600E in papillary thyroid cancers. J Clin Endocrinol Metab. 2018;103:1102–11.
41. Jang MA, Lee ST, Oh YL, Kim SW, Chung JH, Ki CS, et al. Identification of a rare 3 bp BRAF gene deletion in a thyroid nodule by mutant enrichment with 3′-modified oligonucleotides polymerase chain reaction. Ann Lab Med. 2012;32:238–41.